Analysis and outlook of near-industrial PERC solar cells

Pierre Saint-Cast, **Sven Wasmer**, **Johannes Greulich**, **Sabrina Werner**, **Ulrich Jäger***, **Elmar Lohmüller**, **Hannes Höffler** & **Ralf Preu**, Fraunhofer Institute for Solar Energy Systems ISE, Freiburg, Germany

*Now with RENA Technologies GmbH, Gütenbach, Germany

ABSTRACT

This paper presents an in-depth analysis of state-of-the-art p-type monocrystalline Czochralski-grown silicon passivated emitter and rear cells (PERCs) fabricated in a near-industrial manner. PERC solar cells feature a homogeneous emitter on the front side, and an Al_2O_3 passivation layer and local contacts on the rear side. The peak energy conversion efficiencies obtained are 21.1% for a standard anti-reflection coating (ARC), and 21.4% for a double-layer ARC. The loss analysis is based on an extended characterization of the solar cells and of special test samples; this allows the separation of the contributions of each region of the solar cell, including metallization. The impact of the contributions on the open-circuit voltage, the short-circuit current density and the fill factor is determined experimentally. On the basis of the measurements, the devices are numerically simulated, and the free-energy losses are analysed using the simulation model. This simulation allows the calculation of the contribution of the different parts of the solar cell to the efficiency losses. The extensive knowledge of current technology is also the starting point for exploring future technologies for PERC solar cells. An innovative simulation approach allows the future of PERC technology to be mapped out.

Introduction

Passivated emitter and rear cell (PERC) technology [1] using p-type silicon is quickly becoming widespread in crystalline silicon PV, and is expected to establish itself as the industry standard over the next decade. In 2010/2011, major manufacturers began to produce PERC solar cells, with the average energy conversion efficiency in pilot line production using large-area c-Si wafers starting at around 20% [2–3]. In a short period of time, these results could be transferred into mass production [4]. After several years of optimization, the average efficiency has been increased to around 21% in the laboratory and in mass production [5–8]. A few PERC solar cells with an efficiency of 22%, and some with slightly more, have recently been announced by two solar cell manufacturers [9,10]; these, however, are not yet available in mass production.

This paper reports the work carried out in a study of PERC solar cells entirely fabricated at the PV-TEC pilot line [11] at Fraunhofer ISE in a near-industrial manner. The results from several characterization methods applied to solar cells and test samples are combined in order to obtain a detailed analysis of the power losses in the cell. The chosen approach combines experimental evidence and simulation. Previous work has focused only on experimental analysis [12] or simulation [13] in isolation. The approach taken by Fraunhofer ISE, however, combines the realism of experiments with the depth of simulations. These analyses allow a discussion of the strengths and weaknesses of these PERC solar cells, as well as the proposal of further measures to be taken to increase their efficiencies. Going even further, an innovative simulation approach is used to create roadmaps for future PERC technology.

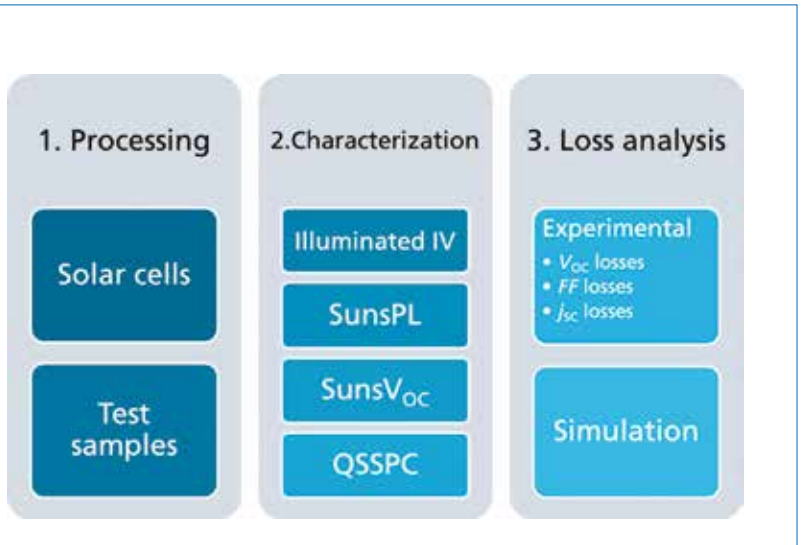

Figure 1. Schematic of the approach used to analyse the losses of Fraunhofer ISE's PERC solar cells.

"The approach taken by Fraunhofer ISE combines the realism of experiments with the depth of simulations."

Loss analysis approach

The focus of the loss analysis is PERC solar cells; PERC cells and fabricated test samples were therefore produced in parallel to independently characterize different regions of the solar cell. The fabrication of the solar cells and the test samples will be presented in the next section.

The solar cells and test samples are

characterized using several techniques, many of which are injection-dependent techniques that allow the analysis of the solar cell close to its actual operating point. Finally, the results generated by the characterization are analysed. What makes this work special is that two different approaches are used simultaneously to analyse the same set of data:

- The experimental loss analysis is a minor modification of the one presented in Wong et al. [12]. The losses are separated into three different types: 1) recombination losses in open-circuit conditions (V_{oc} losses); 2) fill factor (*FF*) losses; and 3) current losses in short-circuit conditions (j_{sc} losses). This loss analysis is closely derived from the experiments.

- To complement the experimental loss analysis, a simulation is carried out. The experimental data from the experimental loss analysis are used to ensure that the simulation is as realistic as possible. Finally, a simulation-based loss analysis is obtained.

A schematic of the loss analysis approach is given in Fig. 1.

Experimental

Solar cell fabrication

The solar cells used in this study were fabricated entirely in the PV-TEC pilot line at Fraunhofer ISE [11]; the process flow is shown in Fig. 2(a). Commercially available industrial tools were used for each of the fabrication processes. Standard-size pseudo-square wafers with an edge length of 156mm were used. The base material was magnetically cast p-type Czochralski-grown silicon (MCz-Si) with a base resistivity ρ_B = 1.4Ωcm. After an alkaline saw-damage removal, the wafers were alkaline textured, and the rear side was chemically polished. The homogeneous emitter was formed in an industrial tube furnace with a diffusion process using $POCl_3$ [14].

Prior to surface passivation, the rear emitter was wet-chemically removed, followed by a cleaning step (SC1/SC2 [15]). The passivation of the rear surface was obtained by an aluminium oxide (Al_2O_3) layer deposited by fast atomic layer deposition (ALD). The ALD process was followed by an outgassing step performed in a tube furnace. A silicon oxide (SiO_x) and silicon nitride (SiN_y) layer stack (Group 1) or a single SiN_y layer (Group 2) served as capping layers. The capping layers were deposited using plasma-enhanced chemical vapour deposition (PECVD). As regards the front-surface passivation, a double-layer anti-reflection coating (ARC) was applied in the case of Group 1, whereas a standard PECVD SiN_z layer was used for Group 2. All the processes employed up to this stage for what is referred to later as the *front end*.

The processes from this stage on, until the finalization of the solar cells, constitute the *back end*; these processes are associated with the formation of the metal contacts. The rear layer stack was locally ablated using a laser process in order to obtain a line-shaped local contact opening (LCO). The front- and rear-side metallizations were applied using screen printing. The front grid featured five busbars, and the rear electrode consisted of full-area screen-printed aluminium (Al). Finally, the contact firing was performed in an industrial conveyor belt furnace. The front and rear cell design is illustrated in Fig. 2(b).

Test sample creation

In order to separate the recombination currents under open-circuit conditions from different parts of the solar cell, test samples were created in parallel with the fabrication of the solar cells. The wafers and the processes used for these samples were the same as for the solar cells, the only difference being the process sequences.

First, the focus was directed on the samples used for the characterization of the front end. After passivation, the samples were fired without metal present on the wafer surfaces. These samples allow the extraction of the implied open-circuit voltage (iV_{oc}), and are referred to as iV_{oc} *samples*. In order to further characterize the front end, three types of symmetric sample were needed. One type (j_{0e} samples) featured the front surface of an iV_{oc} sample on both sides and allowed the extraction of the recombination

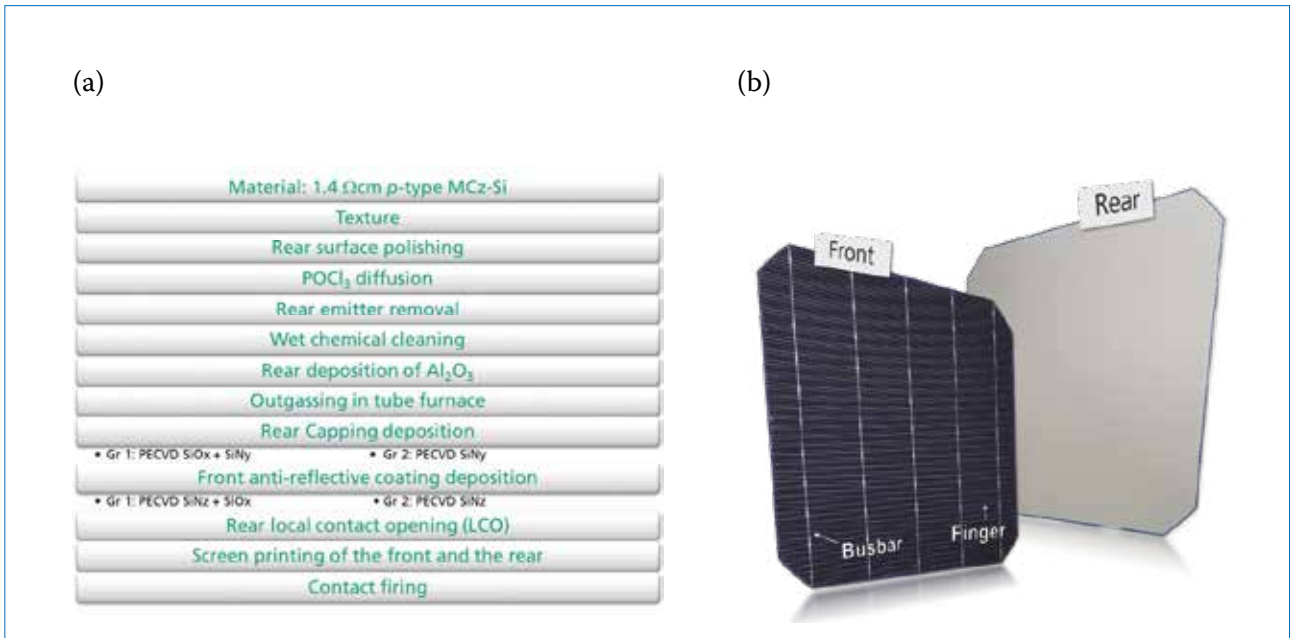

Figure 2. (a) Process flow used for the fabrication of the PERC solar cells at Fraunhofer ISE. (b) The fabricated PERC solar cells, showing the front and rear screen-printed designs.

of the emitter. The second type (S_{pass} samples) featured the rear surface of an iV_{oc} sample on both sides, and allowed the extraction of the recombination due to the rear-side passivation. For the third type, the lifetime of the bulk (τ_{bulk}) was obtained by etching back the passivation layers of the S_{pass} samples using concentrated hydrofluoric acid (HF) and potassium hydroxide (KOH), and then re-passivating both sides with high-quality PECVD AlO_x and subsequent annealing at 425°C.

To study the back end, modified iV_{oc} samples were fabricated:

- iV_{oc} samples with front-side (FS) metallization but no rear-side (RS) metallization. These allowed the loss caused by the front-side metallization to be determined (iV_{oc} + FS Ag).
- iV_{oc} samples with LCO and rear Al. These allowed a determination of the loss caused by the rear contact where a local aluminium back-surface field (Al-BSF) is formed (iV_{oc} + RS LCO).

A schematic of the test sample and the associated recombination in different parts of the solar cell is presented in Fig. 3.

Characterization

Illuminated current–voltage characterization

The current–voltage (I–V) characteristics of the PERC cells were measured using an industrial cell tester. The I–V characteristics of selected samples were independently measured by the Fraunhofer ISE CalLab PV Cells.

The resulting I–V measurements under illumination are summarized in Table 1. Peak energy conversion efficiencies of η = 21.4% and η = 21.1% were obtained for Groups 1 and 2 respectively. The main difference between the groups is the current (j_{sc}), which is higher for Group 1 because of the double-layer ARC and the double capping layers on the rear. The industrial cell tester also includes SunsV_{oc} measurements, I–V measurements in the dark, and busbar-to-busbar resistivity measurements; these will be used later for the analysis of the fill factor. In the following discussion of the work, the characterization and loss analysis focuses on Group 2 (with a single-layer ARC), as it is more representative of current industrial PERC solar cells.

QSSPC, SunsPL and SunsV_{oc} characterization

In order to study the recombination current under open-circuit conditions at 1 sun illumination, and represent it as a function of the injection density for each part of the solar cell, each test sample presented in Fig. 3 needed to be measured by a system with which injection-dependent measurements are possible. The non-metallized samples were measured using quasi-steady-state photoconductance (QSSPC) measurements [16]. The recombination current density j_{rec} as a function of the implied voltage was calculated directly from the measured effective lifetime as a function of the minority-carrier density.

The metallized samples were measured by means of calibrated suns-photoluminescence (SunsPL) [17]. Here, the laser light intensity was varied and measured by a calibrated reference cell. The PL signal was calibrated to implied voltage using two different measurements:

1. The QSSPC measurement of the iV_{oc} samples.
2. The illuminated I–V measurement of the solar cell.

Both of these calibrations yielded very consistent results.

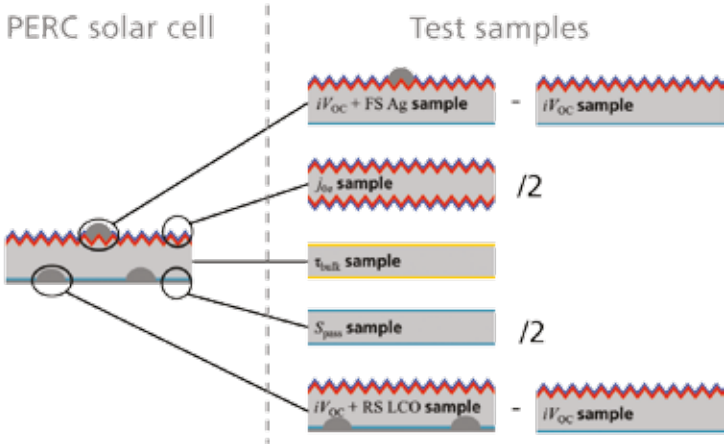

Figure 3. Schematics of the PERC solar cells and of the test samples used for the characterization of the different regions of the cell. To obtain the recombination due to the contacts (front or rear contact), the recombination of the sample without contacts is subtracted from the recombination of a sample with contacts. In order to study the recombination on the front or rear surface, symmetric samples are fabricated whose recombination currents are divided by two, to account for only one surface.

Group		V_{oc} [mV]	j_{sc} [mA/cm^2]	FF [%]	η [%]
1 (double-layer ARC)	Best cell	668	40.0	80.2	21.4*
	Average of 13 cells	664±3	40.1±0.05	80.2±0.4	21.3±0.2
2 (single-layer ARC)	Best cell	665	39.4	80.3	21.1*
	Average of 13 cells	662±5	39.6±0.03	80.1±0.7	21.0±0.3

Table 1. Open-circuit voltage V_{oc}, short-circuit current density j_{sc}, fill factor FF and energy conversion efficiency η for both PERC solar cell groups. The most efficient cell of each group was independently measured at Fraunhofer ISE CalLab PV Cells, and indicated by *.

Finally, the injection-dependent behaviour of the solar cell was obtained using SunsV_{oc} measurements, where the recombination current as a function of the junction voltage was directly measured; therefore, for each test sample, the recombination current was obtained as a function of the implied voltage (Fig. 4). For the experimental loss analysis, only the recombination current at V_{oc} of the finished solar cells (665mV) was used; however, for the simulation-based loss analysis, the entire injection-dependent measurements were taken into account.

Fill-factor-related characterization

The fill factor was first studied by comparing the actual fill factor ($FF \approx 80.1\%$), the pseudo fill factor ($pFF \approx 82.7\%$), and the theoretical maximal fill factor ($FF_0 \approx 83.7\%$) [18]. The FF was determined to have decreased by $2.6\%_{abs.}$ because of resistive losses, and by $1\%_{abs.}$ because of shunt and non-linear recombination as well as possibly inhomogeneous spatial recombination, such as edge recombination (mainly second-diode saturation current density j_{02}). The resistive losses can be further divided using an analytical model of the front-side resistance [19]. The following measured parameters were used as input parameters: the emitter sheet resistance $R_{sh} = 85\Omega/sq.$; the specific contact resistance of the front metal contacts $\rho_c = 3m\Omega cm^2$; and the specific resistance of a metal grid finger $R_{Grid} = 47\Omega/m$. The spreading resistance in the base was obtained by means of an analytical model [20]. The contact resistance at the local rear contacts was neglected, because it is assumed to cause only a gradually vanishing efficiency loss [21].

Short-circuit-current-related characterization

The j_{sc} was studied by measuring the reflectance and spectral response [22]. The shading of the front contacts, the reflectance of the active cell area and the escape light were obtained from the reflection measurements, as described in Thaidigsmann et al. [22]. The emitter recombination was calculated by integrating the internal quantum efficiency in the short-wavelength range ($250nm \leq \lambda \leq 600nm$). The losses corresponding to the bulk and rear recombinations and to the parasitic absorption in the rear metal are determined by performing the same integration in the long-wavelength range ($600nm \leq \lambda \leq 1{,}200nm$). These losses for $600nm \leq \lambda \leq 1{,}200nm$ cannot be separated from one another directly from the measurements alone. The separation of these losses was treated in the simulation part of the loss analysis (see Fig. 5). All losses were weighted with the AM1.5g standard spectrum [23] to obtain a current density.

Loss analysis

Experiment-based loss analysis

For each loss category (recombination at V_{oc}, FF and j_{sc} losses), the losses of the different parts of the solar cell were compared in order to obtain a relative loss in per cent. However, as the losses of different categories cannot be compared with one another, each category needs to be analysed separately. This is the main limitation of this experimental loss analysis, as it

is not possible to obtain the total losses for one specific part of the solar cell. For example, this method allows the calculation of how many per cent of the recombination losses, the *FF* losses and the current losses are accounted for by the front metal grid. However, since the way in which the losses of different categories are related to the total losses is unknown, this method does not allow the calculation of the total influence of the front metal grid on cell efficiency. The relative losses for each category and for each part of the solar cell are shown in Fig. 5.

Simulation-based loss analysis

Numerical simulations of the optics, the special samples and the finished solar cells were conducted using a Sentaurus TCAD; the measurement results of cell Group 2 were used as input to the simulation, and each part of the simulation was compared with the experiment equivalent in order to achieve a realistic model. State-of-the-art physical models [24] were employed. In order to set up the most realistic parameter for the modelling of the PERC solar cell, all the test samples were also simulated for the entire measured range of injection density. The PERC solar cell was then simulated using the acquired calibrated input.

On the basis of these simulations, a free-energy loss analysis was conducted for the finished solar cell. In contrast to the analytical loss analysis, the free-energy loss analysis, including the optical part [25], gives an evaluation of the losses at maximum power point condition and allows the direct comparison of the losses with each other (see Fig. 5).

> "The results from the simulation agreed fairly well with the results obtained experimentally."

The consistency between the experimental and the simulation loss analyses was verified by comparing the distribution of losses between the categories. For the optical losses, the rear parasitic absorption is reflected in the experimental analysis combined with base and rear recombination, and therefore cannot be compared specifically; as for the other optical losses, the measured and simulated distributions differed by less than 3%. For the recombination losses,

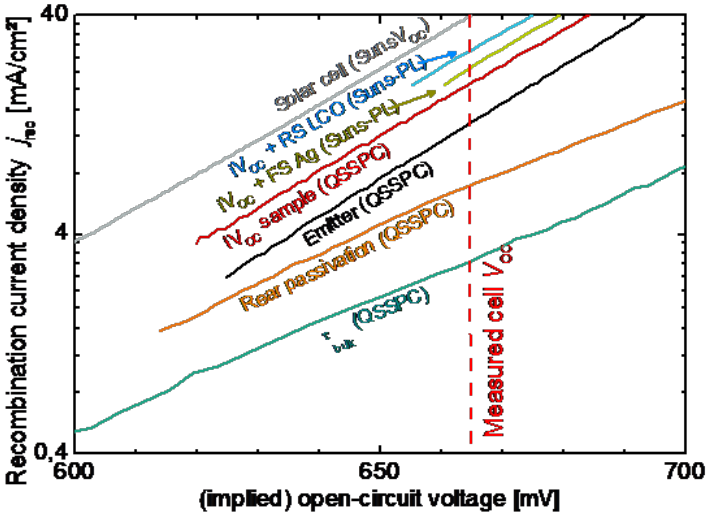

Figure 4. Recombination current density as a function of implied or real open-circuit voltage, for each test sample.

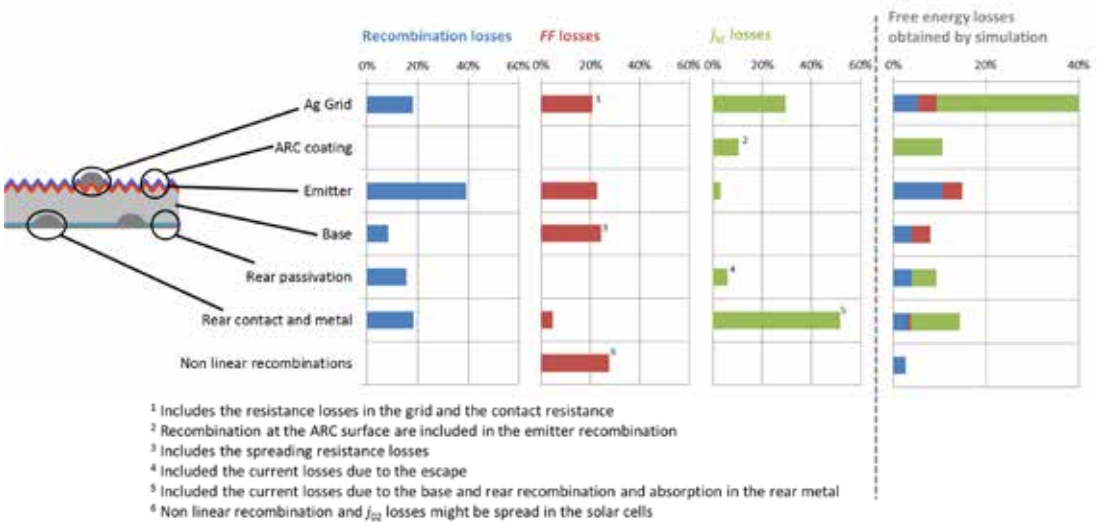

Figure 5. Results of the experiment- and simulation-based loss analyses. For the experiment-based analysis, the recombination, fill factor and current losses are presented separately. For the simulation-based analysis, all the loss categories can be grouped together. This loss analysis focuses on the cell from Group 2 only.

an additional simulation in open-circuit condition was carried out. The measured and simulated distributions of the losses differed by less than 5%, whereas the distributions of the transport losses differed by less than 3%. The highest difference (5%) in loss distribution was thus observed for the recombination losses, which are also the most difficult to characterize. However, it was concluded that the results from the simulation agreed fairly well with the results obtained experimentally (Fig. 5).

Discussion

The main optical losses of the solar cells are due to the front metal reflection and rear absorption, which could be slightly reduced using advanced metallization technologies. The reflectance between the fingers can be decreased using a double-layer ARC (the best cell in this work). However, this approach might not improve the module output power. The recombination on the front side (emitter + front metal grid) is the dominant recombination loss mechanism; this could be reduced by the implementation of a selective emitter. The losses associated with the transport are fairly equally distributed (electron, hole and metal) and represent a small share of the total losses.

In the next section, the focus will be on using simulations to predict the impact of technological developments on the efficiency of PERC cells. With regard to this, a complete loss analysis has been published in more detail in Saint-Cast et al. [26].

Next technological steps

In order to plan the next technology, it is firstly very important to thoroughly understand current technology and its limitations. The work carried out so far has provided a very good and precise knowledge of the status quo, and the model constructed for the calculations relating to the loss analysis is a very good starting point for further simulations. To simulate possible technological improvements, one can start with current technology and proceed to change the parameters corresponding to each improvement in the simulation. Hence, the approach taken here is scenario-based, whereby the improvement that leads to the highest gain in efficiency is iteratively chosen. It is necessary to postulate and simulate different scenarios in order to explore these routes and determine whether or not they can lead to the optimal cell structure in an efficient manner. The downside of this method is that simulation results are only obtained for just a few postulated scenarios, and interesting combinations might therefore remain unexplored.

The obvious solution is then to explore all possibilities. While this might sound very appealing, it would clearly be impossible to achieve, considering the number of simulations required for exploring the entire input space. For example, if 13 variables on five levels are varied in a full-factorial design, this would demand 5^{13} simulations, or more than 1.2 billion simulations in order to cover the input space. Fraunhofer ISE's approach is to simulate monocrystalline p-type PERC cells using a state-of-the-art design of experiment (DoE) and metamodelling approach, formerly also applied to multicrystalline PERC cells [27–29]. It was found that 1,000 simulations are sufficient to preserve the accuracy of the numerical device simulations in the metamodel, which reduces the number of required simulations by a factor of a million. As an example, this kind of arrangement for a three-dimensional space is shown in Fig. 6.

With the application of the metamodel being fairly rapid, it is now possible to iteratively detect the technological improvements that would lead to the highest gain in efficiency. Since the entire input space is readily available, physical and technological constraints on the input parameters (such as series resistance contribution and shading ratio of the front-side metallization, which cannot be varied independently) can be implemented. Furthermore, the distance of the local contacts on the rear side is optimized for every technology in order to obtain a fair comparison in the simulation. The described process leads to a roadmap that anticipates the possibility of producing monocrystalline p-type silicon PERC cells with efficiencies above 23%. Starting with the current technology, the milestones on this roadmap (see Fig. 7) are: the introduction of a selective emitter followed by an improved front metallization, an improved local back-surface field, an improved rear passivation, and finally the use of a double-layer ARC. More details about this approach will be reported in a future publication [30].

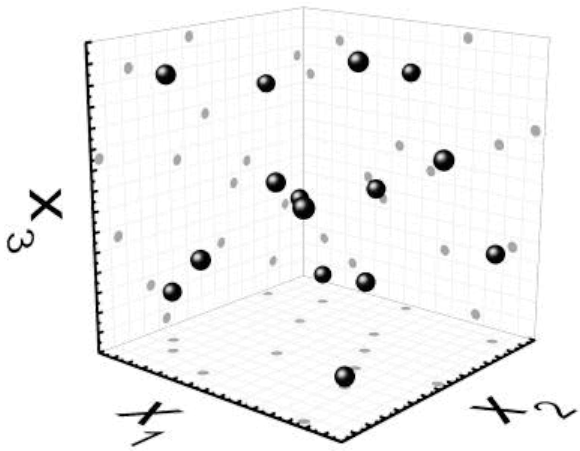

Figure 6. Example of a space-filling DoE for a three-dimensional variable space. The grey points are the projections onto the planes spanned by the axes.

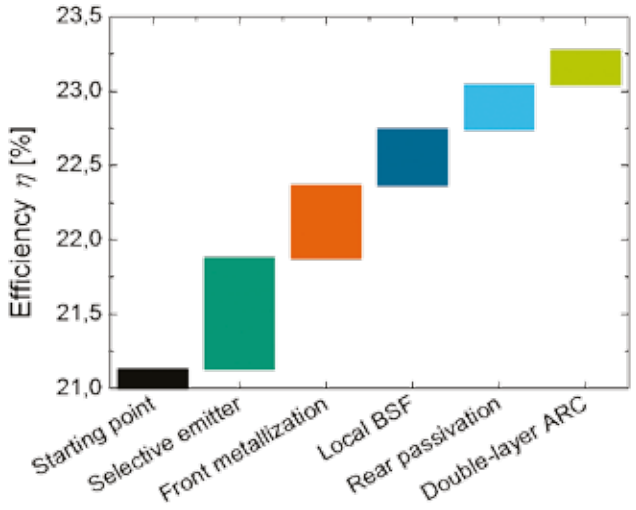

Figure 7. Cell efficiency as a function of the technological improvement for present and future PERC solar cell technology.

"The described process leads to a roadmap that anticipates the possibility of producing monocrystalline p-type silicon PERC cells with efficiencies above 23%."

Summary

The work reported in this paper has provided an extensive loss analysis of PERC solar cells fabricated in the PV-TEC pilot line, with up to 21.4% conversion efficiency. A reliable loss analysis of the current PERC cell technology with homogeneous emitter has been made available thanks to this study. The main losses of the solar cell studied, due first to the front grid and second to the recombination in the emitter, are located on the front surface. This opportunity to build a realistic simulation model of the PERC solar cell was used to advantage; the model allowed a numerically based power loss analysis at the maximum power point. The results were in fairly good agreement with the experimental loss analysis.

With a solid understanding of current technology, a method was developed to explore the effect of technological improvements through simulations. This method allows potential technological improvements of future PERC solar cells to be mapped out on a roadmap. The next stage for improvement is the implementation of a selective emitter, leading to an efficiency close to 22%. Conversion efficiencies of 23.3% could be realized after further improvements to the front metallization, the local rear contact, the rear passivation and the ARC.

Acknowledgements

This work was conducted within the frameworks of the projects CUT-A (0325823) and CUT-B (0325910A), supported by the German Federal Ministry of Economics and Energy (BMWi).

References

[1] Blakers, A.W. et al. 1989, *Appl. Phys. Lett.*, Vol. 55, pp. 1363–1365.
[2] Münzer, K.A. et al. 2010, *Proc. 25th EU PVSEC*, Valencia, Spain, p. 2314.
[3] Engelhart, P. et al. 2011, *Proc. 26th EU PVSEC*, Hamburg, Germany, p. 821.
[4] Tjahjono, B. et al. 2013, *Proc. 28th EU PVSEC*, Paris, France, p. 775.
[5] Neuhaus, H. 2016, PVCellTech Conf., Kuala Lumpur, Malaysia.
[6] Metz, A. et al. 2014, *Sol. Energy Mater. Sol. Cells*, Vol. 120, p. 417.
[7] Dullweber, T. et al. 2014, *Proc. 30th EU PVSEC*, Kyoto, Japan, p. 621.
[8] Gintech 2016, Press Release (Jan. 5), *pv magazine*.
[9] Trina solar 2015, Press Release (Dec. 16), *pv magazine*.
[10] Solar World AG 2016, Press Release (Jan. 14), *pv magazine*.
[11] Biro, D. et al. 2006, *Proc. 21st EU PVSEC*, Dresden, Germany, pp. 621–624.
[12] Wong, J. et al. 2015, *IEEE J. Photovolt.*, Vol. 5, No. 2.
[13] Brendel, R. et al. 2015, *Prog. Photovoltaics Res. Appl.*, DOI: 10.1002/pip.2696.
[14] Werner, S. et al. 2014, *Proc. 29th EU PVSEC*, Amsterdam, The Netherlands, p. 1342.

[15] Kern, W. et al. 1970, *RCA Review*, Vol. 31, pp. 187–205.
[16] Sinton, R.A. & Cuevas, A. 1996, *Appl. Phys. Lett.*, Vol. 69, No. 17, pp. 2510–2512.
[17] Trupke, T. et al. 2015, *Appl. Phys. Lett.*, Vol. 87, No. 9, p. 93503.
[18] Greulich, J. et al. 2010, *Prog. Photovoltaics Res. Appl.*, Vol. 18, No. 7, pp. 511–515.
[19] Fellmeth, T. et al. 2014, *IEEE J. Photovolt.*, Vol. 4, No. 1, pp. 504–513.
[20] Saint-Cast, P. 2012, Ph.D. dissertation, Constance University, Germany, p. 61.
[21] Müller, M. et al. 2014, *J. Appl. Phys.*, Vol. 115, p. 084505, DOI 10.1063/1.4867188.
[22] Thaidigsmann, B. et al. 2009, *Proc. 24th EU PVSEC*, Hamburg, Germany, pp. 2056–2059.
[23] IEC 60904-3:2008, "Photovoltaic devices: Part 3. Measurement principles for terrestrial photovoltaic (PV) solar devices with reference spectral irradiance data".
[24] Altermatt, P.P. 2011, *J. Computat. Electron.*, Vol. 10, pp. 314–330.
[25] Greulich, J. et al. 2013, *J. Appl. Phys.*, Vol. 114, No. 20, p. 204504.
[26] Saint-Cast, P. et al. 2016, "Analysis of the losses of industrial-type PERC solar cells", *physica status solidi (a)*, DOI 10.1002/pssa.201600708.
[27] Wasmer, S. et al. 2016, "Understanding process-related efficiency variations in mc-Si PERC cells", *Photovoltaics International*, 31st edn, pp. 43–52.
[28] Wasmer, S. et al. 2016, "Impact of material and process variations on the distribution of multicrystalline silicon PERC cell efficiencies", *IEEE J. Photovolt.* (10.1109/JPHOTOV.2016.2626145).
[29] Müller, M. et al. 2014, "Sensitivity analysis of industrial multicrystalline PERC silicon solar cells by means of 3-D device simulation and metamodeling", *IEEE J. Photovolt.*, Vol. 4, No. 1, pp. 107–113.
[30] Wasmer, S. et al. 2017 [forthcoming], 7th Int. Conf. Crystall. Si. Photovolt., Freiburg, Germany.

About the Authors

Pierre Saint-Cast received his M.Sc. in micro- and nanoelectronics from Joseph Fourier University, Grenoble, France, and his engineering degree from the Polytechnic Institute of Grenoble, both in 2007. In 2012 he was awarded a Ph.D. by the University of Konstanz, Germany. Since 2008 he has been with Fraunhofer ISE, where his research interests include the development of passivation layers for solar cell applications, and the processing, analysis and analytical modelling of PERC solar cells.

Sven Wasmer studied physics at the University of Freiburg, Germany, and received his diploma in 2013, in collaboration with Fraunhofer ISE. He is currently working towards his Ph.D. at Fraunhofer ISE, with a topic of the characterization and simulation of process variations in solar cell production.

Johannes Greulich studied physics in Heidelberg and in Freiburg, Germany, where he received a diploma degree in 2010. In 2014 he obtained his Ph.D. in physics from the University of Freiburg for his work on the simulation and characterization of novel large-area silicon solar cells. Since 2015 he has been head of a research team at Fraunhofer ISE, working on inline solar cell characterization, device simulation and image processing.

Sabrina Werner studied physics at the University of Freiburg, Germany, and received her diploma degree in 2011. Since 2009 she has been with Fraunhofer ISE, working in the PV production technology and quality assurance division. Her research interests include the investigation and improvement of high-temperature processes and passivated solar cells.

Ulrich Jaeger received his diploma degree in physics in 2008 from the Technical University of Darmstadt, Germany. From 2008 to 2013 he worked at Fraunhofer ISE, both as a Ph.D. student and a postdoctoral researcher in the PV production technology and quality assurance division, on the topic of laser doping for the industrial fabrication of crystalline silicon solar cells and as a project manager for the development of passivated silicon solar cells. Since 2016 he has been with RENA Technologies GmbH, where he is involved in sales and business development for production equipment for PV devices.

Elmar Lohmüller studied physics at the University of Tübingen, and at Nelson Mandela Metropolitan University, Port Elizabeth, South Africa. He received his diploma degree in 2010 for his work at Fraunhofer ISE on the development of p-type MWT-PERC solar cells. He then worked on the development of n-type MWT solar cells, for which he received a Ph.D. from the University of Freiburg in 2015. He is currently a researcher at Fraunhofer ISE, where he focuses on the development of p-type PERC solar cells.

Hannes Höffler studied physics at the University of Freiburg, Germany, and received his diploma in 2010. In 2015 he was awarded a Ph.D. in physics by the University of Freiburg for his work on luminescence imaging and its applications in the processing of silicon solar cells in an industrial environment. He is currently responsible for the offline characterization laboratory in the PV production technology and quality assurance division at Fraunhofer ISE.

Ralf Preu is the director of the PV production technology and quality assurance division at Fraunhofer ISE in Freiburg, Germany, and also teaches photovoltaics at the University of Freiburg. He studied physics at the universities of Freiburg and Toronto, as well as economics at the University of Hagen, Germany, and has a Ph.D. degree in electrical engineering. He joined Fraunhofer ISE in 1993 and has worked in different fields in PV, including system monitoring, and silicon solar cell and module technology, characterization and simulation. His main focus is on the R&D of advanced silicon solar cell technology and its transfer to industrial production.

Enquiries

Pierre Saint-Cast
Fraunhofer Institute for Solar Energy Systems ISE
Heidenhofstraße 2
79110 Freiburg, Germany

Tel: +49 (0)761 4588 5480
Email: pierre.saint-cast@ise.fraunhofer.de